PERIODICA POLYTECHNICA SER. TRANSP. ENG. VOL. 30, NO. 1–2, PP. 93–109 (2002)

CUTTING PARAMETERS DEFINITION FOR KINEMATIC OPTIMISATION OF SPIRAL BEVEL GEARS

Márk LELKES*, Daniel PLAY** and János MÁRIALIGETI*

*Department of Vehicle Parts and Drives
Budapest University of Technology and Economics
H–1111 Budapest, Bertalan L. utca 2, Z ép. Hungary
Phone: +36 1 463–1739, Fax: +36 1 463–1653
e-mail: lelkes@kge.bme.hu, marial@kge.bme.hu
**Federal-Mogul Opérations France S.A.S. Sintered Products
Iles Cordées, 38113 Veurey Voroize, France
Phone: +33 4 76 53 79 64, Fax: +33 4 76 53 79 97
e-mail: daniel_play@eu.fmo.com

Received: April 16, 2002

Abstract

The contact analysis of uniform tooth height epicyclical spiral bevel gears stemming from Klingelnberg's Cyclo-Palloid System has an important role in preliminary design. The simultaneous generation of gear surfaces and contact simulation is the basis of the analysis. A numerical program for theoretical contact identification has been developed. Longitudinal settings of the contact patterns or contact across the surfaces from tooth root to tooth top were obtained as a function of machine settings. The influence of each cutting parameter was isolated and is discussed for kinematic optimization.

Keywords: gear design, spiral bevel gears, kinematic optimization, contact analysis.

1. Introduction

The high performance gear transmissions require increasingly fine definition of tooth gear geometry in order to ensure satisfactory kinematics and dynamic performances. The spiral bevel gear behaviour is particularly sensitive to the initial geometry of the tooth surfaces. In order to take into account significant machining parameters and to control tooth surface after machining [FONG, GOSSELIN et al. (2000), KAVASAKI et al, REMOND et al., ZHANG et al. (1994)] many authors have attempted to formalize the theory of geometry definition [FONG, GOSSELIN et al. (1993), HANDSCHUH et al., LITVIN et al., MÁRIALIGETI et al., ZHANG et al. (1994)]. In the practice, the contact pattern must be situated in the centre of the tooth surface. In addition, satisfactory contact conditions and the lowest possible kinematic error are required during the motion. Thus, flank corrections must be made to modify the tooth surface in tooth width direction (toe-heel) and profile direction (top-root) or the twist of the tooth flank can also be imagined [LITVIN et al., MÁRIALIGETI et al., STADTFELD et al.]. Any kind of combination of these corrections is applied for the geometry modifications on the basis of closely related

machining parameters. It is not easy to predict the geometric changes of tooth surfaces. Moreover, the meshing of the two tooth surfaces of the pinion and gear can be modified and interactions of gear and pinion parameters must be also considered.

In the Klingelnberg's Cyclo-Palloid System, a continuous cutting procedure is achieved in which tooth surfaces are basically conjugated [LITVIN], both the concave and the convex sides of the tooth surfaces are machined simultaneously. The finishing points of the cutter edge trace the longitudinal shape of the tooth surface. The extended epicycloid is obtained by a rolling over motion (*Fig.1*). In the figure, constant bevel pinion tooth height can be observed and the extended epicycloid path gives the curved shape of the teeth. Note that a reference point *P* is defined as an intersection of the mean cone distance and the extended epicycloid. Obviously, the shape and the orientation of cutter edges govern the final tooth surfaces. In order to avoid either the contact of extreme parts of the surface (top, heel or toe contact) or the discontinuous function of the transmission error [FONG et al., GOSSELIN et al. (2000), LELKES et al (2001), LELKES et al (2000), LITVIN et al., STADTFELD et al., ZHANG et al. (1994), ZHANG et al. (1995)] the tooth surfaces are mismatched. This is also aiming at obtain a stabilized bearing contact.

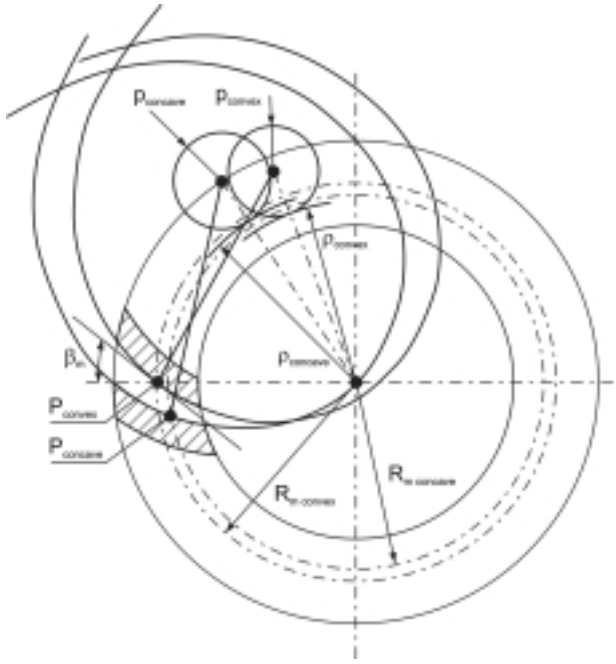

Fig. 1. Klingelnberg's Cyclo-Palloid System

The contact pattern is controlled and evaluated after machining. It should match design criteria, such as centring in the middle of the surface otherwise repositioning is needed. The varying machine settings and cutting parameters have

two main types of corrections for changing tooth flank geometry. The corrections of the surface for the contact pattern that contain the conjugated points on the modified tooth flank [LITVIN et al., STADTFELD et al.] are considered in two directions on the gear tooth surface either along the length direction or along height direction. In tooth length corrections the radius of the cutter head is varied (*Fig.2*). Thus the curvature of the longitudinal shape of the convex side of the generating crown gear is modified. The curvature increases while the radius is reduced. This correction also changes the machine distance. A curved cutter edge is introduced, as opposed to the originally straight-line cutter edge, in order to modify the tooth surface in height direction (*Fig. 3*). Due to the conjugated points, both corrections have zero kinematic error. The contact areas are located across the surface in tooth length direction correction, there is no bias. On the contrary, for tooth height corrections, longitudinal contact areas appear. The line contact of the conjugated profiles becomes point contact. Corrections in both directions support only one conjugated point (mean point), resulting in a parabolic shape for kinematic error function. Consequently, several machine-setting modifications can be considered to optimize the location of the contact pattern and the level of the kinematic error.

Our purpose is to take into account the significant cutting parameters and their influences on the contact characteristics, finally, to make comparisons of various machine settings in order to achieve contact optimization, moreover to define a flexible design method for epicyclical spiral bevel gears.

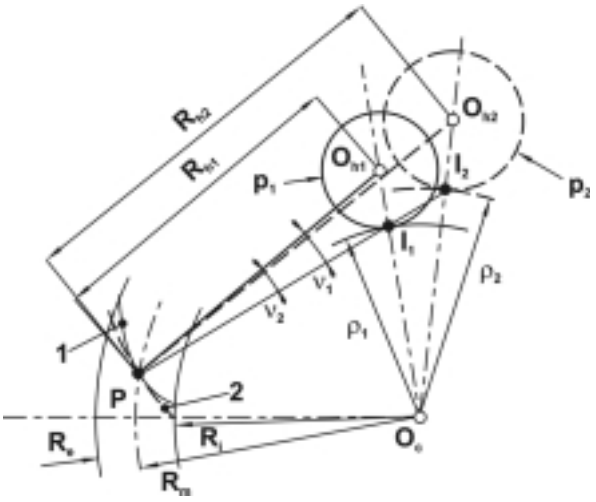

Fig. 2. Machine settings for tooth length direction correction

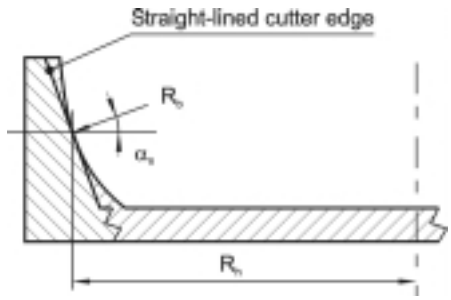

Fig. 3. Machine settings for tooth height direction correction

2. Mathematical Model of the Generation Process

The tooth surface generation process is presented for the pinion tooth surface generation. The geometry of the cutter edge (*Fig. 4*) is described in the co-ordinate system S_b, the generating point P of the cutter edge is represented by the radius vector $\mathbf{r}_b(t)$. The co-ordinate system S_b is rotated around axis z_t with angle ν. The angle ν is a basic angle when the cutter edge plane is directed towards the instantaneous axis I of rotation (*Fig. 2*).

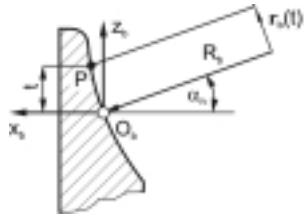

Fig. 4. Cutter edge geometry for pinion generation

The auxiliary co-ordinate system S_t is rigidly connected to the co-ordinate system S_h of the head cutter (*Fig. 5*). The radius of the head cutter is $R_h = \overline{O_t O_h}$. The co-ordinate system S_h performs a rotation φ about axis z_u. The auxiliary co-ordinate system S_u is rigidly connected to another auxiliary co-ordinate system, S_v. The machine distance $M_d = \overline{O_u O_v}$ links the two co-ordinate systems. The co-ordinate system S_v rotates about axis z_c, φ_a being the current rotation angle. The co-ordinate system S_c is attached to the generating crown gear. Angles φ and φ_a are related by *Eq.* (1) where p and ρ are respectively the radius of the rolling circle and the base circle.

$$\frac{\varphi}{\varphi_a} = \frac{\rho}{p}. \tag{1}$$

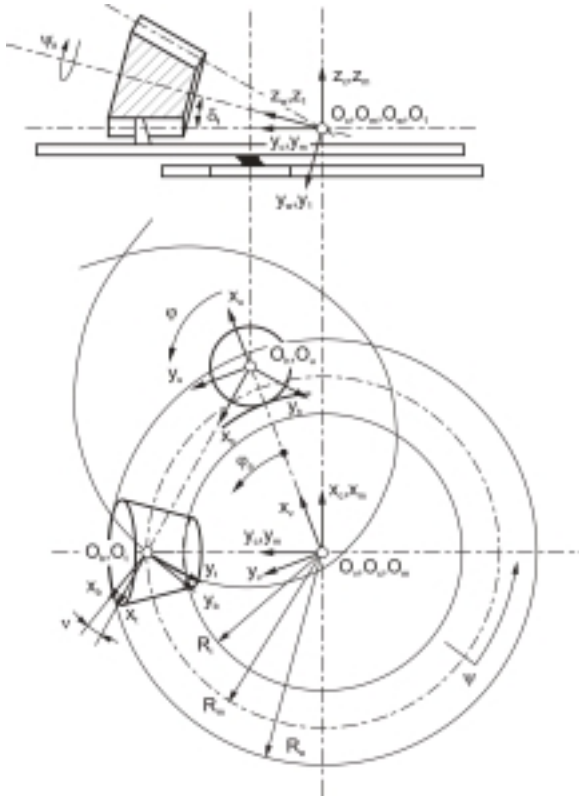

Fig. 5. Co-ordinate systems for gear tooth surface generation

The generating crown gear gives the tooth surface (*Fig.*5) and the co-ordinate system S_c rotates about axis z_m by an angle of rotation ψ. Pinion co-ordinate system S_1 rotates simultaneously about axis z_w, with angle ψ_a. The installation position of the co-ordinate system S_w, in relation with the co-ordinate system S_m, is determined by pitch angle δ_1, measured clockwise. The relation between these two angles, ψ, ψ_a, is given in *Eq.* (2). The instantaneous axis of rotation is the axis y_m.

$$\frac{\psi}{\psi_a} = \sin \delta_1. \tag{2}$$

2.1. Obtaining Tooth Surfaces

Tooth surface generation modelling is realised by describing the movement of cutter edge points in the co-ordinate system of the pinion (or gear) to be generated, via successive transformations between the different co-ordinate systems described

above. These transformations are governed by the relative rotations during cutting. During these matrix transformations and calculations, the tooth surfaces of the generating crown gear are represented in its own co-ordinate system by the radius vector $\mathbf{r}_c(\varphi_i, t_i)$. When the generating motion occurs, the family of the tooth gear surfaces is represented in the co-ordinate system of the pinion or the gear. The family of the gear tooth surfaces $\mathbf{r}_i(t_i, \varphi_i, \psi_i)$ is described by the matrix *Eq.* (3), where $\mathbf{r}_i$ is the location vector of a tooth surface point, and matrices $\mathbf{M}_{ij}$ stand for the individual co-ordinate transformations [LITVIN]. The tooth surface depends on the parameter t_i of the generating point of the cutter edge, the rotation angle φ_i of the cutter head and the rotation angle ψ_i of the generating crown gear. The parameter t_i can be eliminated, as it depends on the two other parameters [KAVASAKI et al.], *Eq.* (4).

To find the unique point on each generated surface, which belongs to the tooth surface of the pinion, corresponding values of parameters t_i, φ_i, ψ_i, belonging to the real generating position are to be determined. This is done by the fact, that the generating position of the generating gear is situated on the normal vector of the surface generating crown gear, furthermore, this normal vector passes through the instantaneous axis of rotation [LITVIN et al.]. The set of equations is solved by a numerical Gauss iteration procedure [POPPER] and used for the further contact investigations.

$$\mathbf{r_i}(t_i, \varphi_i, \psi_i) = \mathbf{M}_{iw}(\psi_i) \cdot \mathbf{M}_{wm} \cdot \mathbf{M}_{mc}(\psi_i) \cdot \mathbf{M}_{cv}(\varphi_i) \cdot \mathbf{M}_{vu} \cdot \mathbf{M}_{uh}(\varphi_i) \cdot \mathbf{M}_{ht} \cdot \mathbf{M}_{tb} \cdot \mathbf{r}_b(t_i) \tag{3}$$

$$t_i = t(\varphi_i, \psi_i). \tag{4}$$

3. Kinematic Error

The kinematic error is a well-known parameter used to qualify the kinematic excitation of gear pair [FONG et al., GOSSELIN et al (2000), LITVIN et al., ZANG et al. (1994)]. The kinematic error is zero, if driven gear rotation angle $\phi_2(\phi_1)$ in *Eq.* (5), equals the calculated value obtained form the mean transmission ratio and the driving pinion rotation angle ϕ_1, where Z_1 and Z_2 represent the number of pinion and gear teeth, respectively.

$$\phi_2(\phi_1) = \frac{Z_1}{Z_2}\phi_1, \tag{5}$$

where the rotation angle $\phi_2'(\phi_1)$ of the driven part differs from the ideal angle ϕ_2, a kinematic error $\Delta\phi_2(\phi_1)$ is calculated in *Eq.* (6). When the angle of rotation of the driven part is lower than the value calculated from the transmission ratio, then the kinematic error is considered to be negative.

$$\Delta\phi_2 = \phi_2'(\phi_1) - \phi_2(\phi_1). \tag{6}$$

The contact between theoretically conjugated surfaces gives zero kinematic error. Obviously, the modified gear surfaces give new results. Zero kinematic error level can also be achieved when contacts are made between a basis tooth surface and a tooth length or a tooth height corrected surface.

4. Contact Analysis

The contact simulation is based on the theory of continuous tangency of contacting surfaces and achieved by the simultaneous generation of the main contact surfaces, such as the convex surface of the pinion and the concave surface of the gear flank. The contacting surfaces are described in a fixed co-ordinate system satisfying the meshing equations. The contacting surfaces have common points in contact position (*Eq.* (7)) and the normal unit vectors of the surfaces in this point are equal and opposite (*Eq.* (8)).

Vector equations (7) and (8) supply six independent scalar equations. As far as the normal unit vectors are used, the number of meshing equations for pinion and gear tooth surface generation are also considered as being capable of simulating contact with any kind of machine-settings. Thus, six unknowns ($t_1, \varphi_1, \psi_1, t_2, \varphi_2, \psi_2$) describe the surfaces of the pinion and the gear. From the angles of rotation (ϕ_1, ϕ_2) of the mating gear pair, ϕ_1 is chosen as an input parameter. Parameters t_1 and t_2 could be eliminated, by referring to *Eq.* (4) but for complete non-linear equation system, these parameters are taken into account. Finally, a system of seven non-linear equations is solved by an iterative numerical procedure. Then the characteristics during the contact i.e. the level of the kinematic error, size and shift of the contact pattern are obtained.

$$\mathbf{r}_{s1}(t_1, \varphi_1, \psi_1, \phi_1) - \mathbf{r}_{s2}(t_2, \varphi_2, \psi_2, \phi_2) = 0, \tag{7}$$

$$\mathbf{n}_{s1}(t_1, \varphi_1, \psi_1, \phi_1) + \mathbf{n}_{s2}(t_2, \varphi_2, \psi_2, \phi_2) = 0. \tag{8}$$

5. Determination of Contact Pattern

In the case of a loaded tooth contact, surface deformation occurs and contact ellipses can be calculated by using the Hertzian theory of contact. During the motion of gear pairs, ellipse areas are displaced and a contact pattern is obtained. Since only the kinematic of solid bodies is investigated in this study, contact simulation is replaced by a geometric approximation of contact ellipses, considered with a theoretical offset of the tooth surfaces. In practice, the method is based on the determination of the distance between the tooth surfaces in contact. Note that the distances between contacting surfaces are small. Consequently, the calculation of surface distances is approximated by determining the radius vectors. More specifically, for a given contact position, the tooth surfaces are fixed and presented in co-ordinate system S_3

(*Fig. 6*). In the vicinity of contact point P_{sj}, successive cutting planes perpendicular to axis z_s are considered (*Fig. 7*). In each plane, two points are defined in such a way that the distance $P_{s1j}P_{s2j}$ equals 10 μm and the length of their position vectors is equal to each other: $\left|\mathbf{r}_{s1j}\right| = \left|\mathbf{r}_{s2j}\right|$.

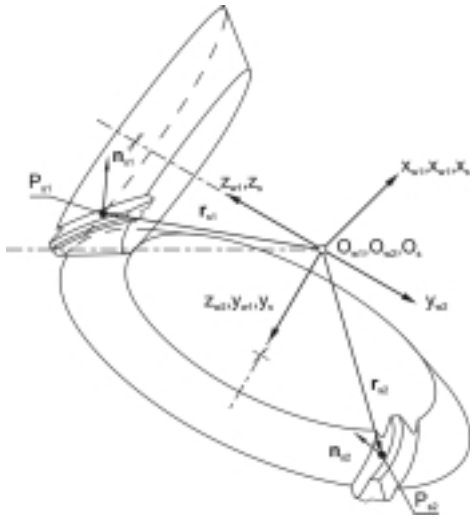

Fig. 6. Co-ordinate systems for contact conditions

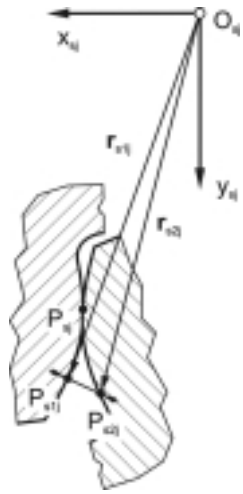

Fig. 7. The determination of the contact ellipse in the plane perpendicular to axis z_{sj}

6. The Presentation of the Results

In all cases the contact patterns are presented on the pinion surface (*Fig.8*). The contact line is composed of instantaneous contact points (thick line in the *Fig.8*). The contact ellipse is simplified by a line segment, which is corresponding to the major axis of the contact ellipse. Obviously, the middle of the segment is situated on the contact line. The extreme lines define the contact pattern. The active part of the contact pattern is defined by the entry and the exit of the mating tooth pair in contact during rotation. The bias of the contact pattern is the extension of the contact line in axis x direction (*Fig. 8*).

Corrections in tooth length direction (case A), in tooth height direction (case B) and corrections in both directions (case C) are considered for the pinion tooth surface. In case of corrections in both directions several machining parameters are examined for kinematic optimization.

In cases A and C, the point M is the intersection of the contact line with the mid pitch cone. In case B, point M is given by the intersection of the contact line with the mid back cone. Consequently, point M is situated in tooth surface zone and will be located by (x, y) co-ordinates whose co-ordinate system has its origin in the central point C. In all cases the displacement of the contact pattern is described by the distance between the point M of the contact line and the central point C of the tooth surface (*Fig. 8*), given by intersection of pitch or mid back cones. If the corrections are applied in tooth length, height or in both directions the points M and C are in the same position. In all cases, a zero kinematic error and contact width w of the contact pattern were defined at point M of the contact pattern along the contact line.

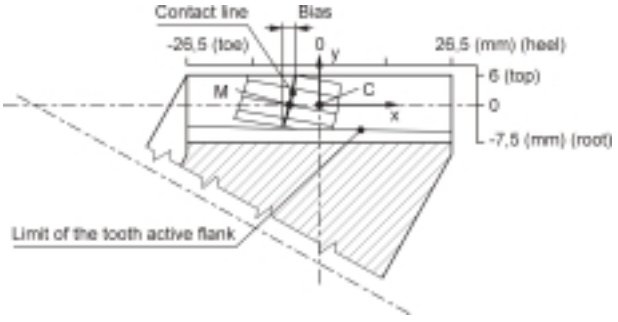

Fig. 8. Visualization of the contact pattern

7. Method of Investigation and Results

Initial data are provided for common parameters (*Table 1*) and also for different settings in the case of pinion (*Table 2*) and gear (*Table 3*).

In case of any correction applied on a tooth surface, the contact will be fundamentally changed. For example, an initial line contact of the conjugated tooth surfaces can become a point contact.

Table 1. Dimensions of spiral bevel gears

		Pinion	Gear
Number of teeth Z		19	34
Shaft angle	(°)	90	
Pitch cone angle	(°)	29.197	60.803
Spiral angle	(°)	29.686	
Hand of spiral		LH	RH
Mean cone distance R_m	(mm)	136.74	136.74
Face width	(mm)	53	53
Pressure angle α_n	(°)	20	20
Normal module	(mm)	6.1	6.1
Number cutter group		5	5

Table 2. Parameters of cutter and machine settings for pinion convex side

		Case A	Case B	Case C
Cutter curvature R_b	(mm)	∞	509.634	509.634
Cutter head radius R_h	(mm)	135	137.4	135
Machine distance M_d	(mm)	149.595	150.683	149.595
Base circle radius ρ	(mm)	132.576	133.54	132.576
Rolling circle radius p	(mm)	17.019	17.143	17.019

Table 3. Parameters of cutter and machine settings for gear concave side

Cutter curvature R_b	(mm)	∞
Cutter head radius R_h	(mm)	137.4
Machine distance M_d	(mm)	150.683
Base circle radius ρ	(mm)	133.54
Rolling circle radius p	(mm)	17.143

The contact characteristics can be influenced as a function of the radius of the cutter edge and the radius of the cutter head. The bias of the contact pattern is increasing as a function of the radius of the cutter edge as it is reduced, thus the

contact line approaches to the pitch cone. On the contrary, as the radius of the cutter head is increased, the contact line approaches to the pitch cone.

7.1. Tooth Length Direction Corrections

In the tooth length direction correction, case A, no kinematic error occurs on the section *b* (*Fig. 9b*) of the tooth surface because the conjugated points stay along a single conjugated line. An initial type of the contact across the tooth surface is occurred (*Fig. 9*). The top contact of the mating gears is examined, sections *d* (top section of the gear is in contact) and *c'* (top section of the pinion is in contact) in *Fig. 9a*. The contact of these parts of the tooth surfaces induces high level of the kinematic error.

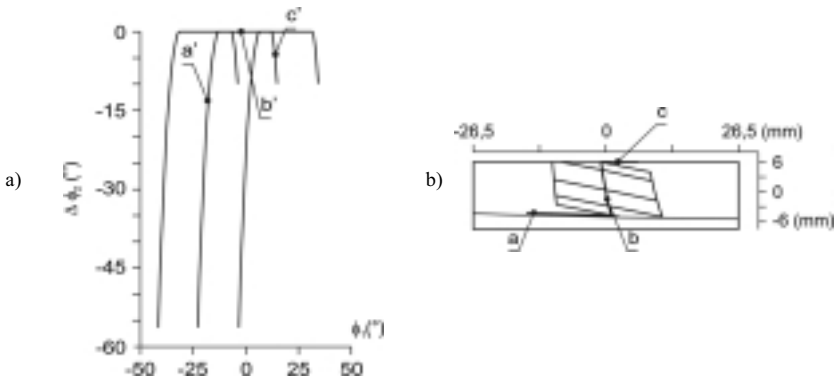

Fig. 9. In tooth length correction, kinematic error (a), contact pattern (b), case A

Table 4. Values of width and bias of the contact pattern

	Case A	Case B	Case C
Contact pattern width w (mm)	21.240	29.301	16.834
Contact pattern bias b (mm)	2.023	53	28.527

7.2. Tooth Height Direction Corrections

In case of this correction (case B) zero kinematic error occurs that could be also traced back to the conjugated points. The contact pattern has a longitudinal shape (*Fig. 10b*), which remains unchanged during the modifications. The toe and heel

contact of the mating gears is examined, sections a' (the toe section of the pinion is in contact) and c' (heel section of the pinion is in contact) are in *Fig. 10a*. The high level of the kinematic error is induced if the contact is realised on the toe or heel section of the tooth surface.

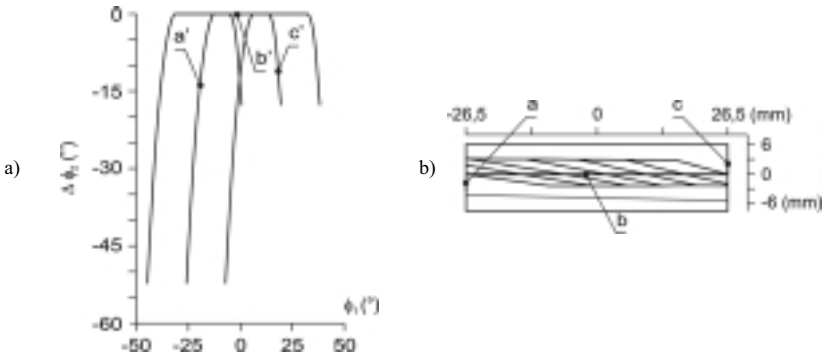

Fig. 10. In tooth height correction, kinematic error (a), contact pattern (b), case B

7.3. Corrections in Both Directions, Optimization of the Kinematics

The tooth flank is corrected in both directions (case C) to optimize kinematics. We only have one remaining conjugated point of the contacting tooth surfaces. The kinematic error function has a quasi-parabolic shape (*Fig. 11a*). A new contact line is a result of the influence of the two parameters and it is situated as a result of two opposite cases (cases A and B). In the initially examined machine settings, a diagonal contact pattern is obtained.

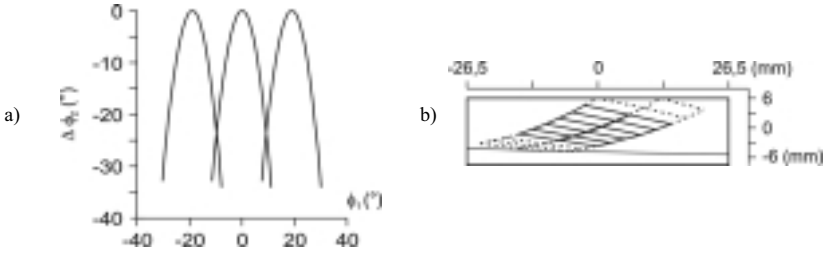

Fig. 11. Tooth surface correction in both directions, kinematic error function (a), contact pattern (b), case C

The localisation of the contact line can be influenced by the cutter edge radius

(*Fig. 12*) and the cutter head radius variation (*Fig. 13*). As the cutter edge radius is reduced, the contact line is approaching to the pitch cone and the maximum kinematic error is increasing. For the other modification, the maximum kinematic error is reducing if the cutter head radius is increased, furthermore the contact line is approaching to the pitch cone. Thus, the maximum kinematic error is influenced in opposite way. Furthermore, the same bias and contact line can be achieved by different modifications (*Table 5* and *6*). A maximum kinematic error surface is computed as a function of the cutter edge radius and the cutter head radius (*Fig.14*). Several machine-settings are proposed for a prescribed maximum kinematic error value (*Table 7*). The localisation of the contact line varies from across the tooth surface to a longitudinal shape (*Fig. 15*).

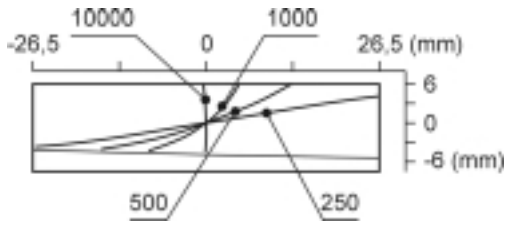

Fig. 12. The localization of the contact line in function of the radius of the cutter edge R_b at $R_h = 135$ mm

Table 5. The bias of the contact pattern in function of the radius of the cutter edge R_b at $R_h = 135$ mm

R_b (mm)	b (mm)	$\Delta\phi_{2\max}$ ($''$)
10000	−0.330	−1.928
1000	13.844	−14.918
500	29.127	−23.877
250	53	−34.011

8. Conclusions

The improvement and optimization of the gear behaviour can be achieved if the influences of machining parameters are known and selected in particular for complex gear systems such as Klingelnberg's Cyclo-Palloid gears. A kinematic approach has been applied to model the cutting process. All significant cutting parameters are

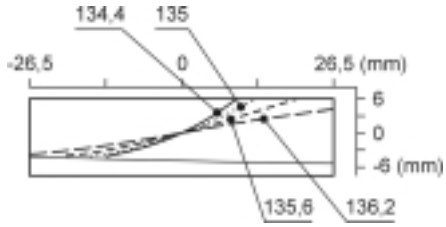

Fig. 13. The localization of the contact line in function of the radius of the cutter head R_h at $R_b = 500$ mm

Table 6. The bias of the contact pattern in function of the radius of the cutter head R_h at $R_b = 500$ mm

R_b (mm)	b (mm)	$\Delta\phi_{2\max}$ ($''$)
136.2	53	−17.330
135.6	40.406	−21.214
135	29.127	−23.877
134.4	22.790	−25.814

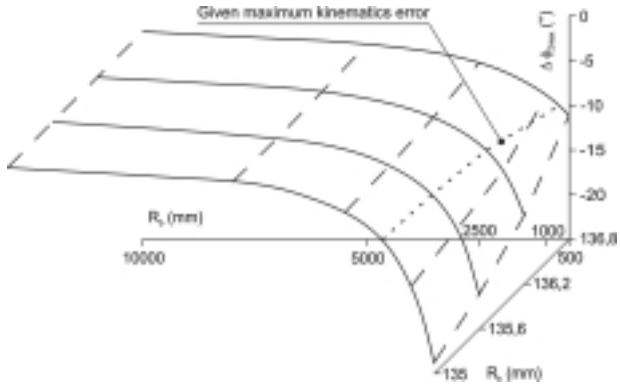

Fig. 14. The values of the maximum kinematic error

taken into account. Thus, the influence and interactions of machining parameters must be known in details and formalized to optimize the kinematics performances. The following conclusions can be drawn:

- A simulation method is presented for the flexible parameter variation to determine the tooth flank geometry, the kinematic error level, and the contact

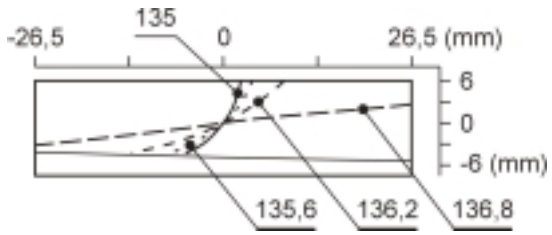

Fig. 15. The localization of the contact line in function of the radius of the cutter head and the cutter edge, the maximum kinematic error is given to 10″

Table 7. The corresponding radius and bias of the cutter head and the cutter edge at 10″ maximum kinematic error

R_h (mm)	R_b (mm)	b (mm)
136.8	711.821	53
136.2	1344.115	21.494
135.6	1551.045	11.783
135	1654.946	7.771

pattern. Tooth surface corrections effects (in tooth length direction, in tooth height direction and both directions) are defined, as well as their interactions are calculated and discussed, based on the developed model.

- It was demonstrated that the radius of the cutter edge and the radius of the cutter head influence the bias variation of the contact pattern.
- A maximum kinematic error surface is determined as a function of the parameters mentioned.
- Based on simulation calculations, various localizations of the contact pattern with a constant maximum kinematic error are obtained.

This study presents a kinematic optimization, which is based on the comparison and qualification of various machine-setting parameters. The purpose of the further studies is to formalize the knowledge on the Klingelnberg gear behaviour, that will make it possible to take into account the tooth flank deformations and the gear contact load sharing.

Acknowledgements

We thank the French Research Ministry and the Hungarian Ministry of Education (grant no.: FKFP 0240/97), as well as the Ganz Dawid Brown Transmission Co., Budapest, for

supporting the present collaborative research program. Special thanks are also due to the National Institute of Applied Sciences in Lyon and the Budapest University of Technology and Economics for the collaborative PhD. Student facilities.

Nomenclature

b	bias
C	mean point of tooth surface
I	instantaneous centre of rotation
M	mean point of the contact line
$\mathbf{M}$	matrix of the co-ordinate transformation
M_d	machine distance
$\mathbf{n}$	normal vector
P	generating point of the cutter edge
p	rolling circle radius
R_b	radius of the cutter edge
R_h	radius of the cutter head
R_m	mean cone distance
$\mathbf{r}$	position vector
t	parameter of the generating point of the cutter edge
w	width of the contact pattern
Z	number of teeth for gear
α_n	pressure angle
$\Delta\phi$	kinematic error
δ	pitch cone angle
κ	rotation of the cutter edge
ν	basic rotation of the cutter edge
ρ	base circle radius
φ	rotation angle for the cutter head
ϕ	rotation angle for the gear during contact
ψ	rotation angle for the generating gear
ψ_a	rotation angle for the gear during generation
1	for the pinion
2	for the gear

References

[1] FONG, Z. H., Mathematical Model of Universal Hypoid Generator with Supplemental Kinematic Flank Correction Motions, *ASME Journal of Mechanical Design*, **122** (2000), pp. 136–142.

[2] FONG, Z. H. – TSAY, C. B., Kinematical Optimisation of Spiral Bevel Gears, *ASME Journal of Mechanical Design*, **114** (1992), pp. 498–506.

[3] GOSSELIN, C. J. – CLOUTIER, L., The Generating Space for Parabolic Motion Error Spiral Bevel Gears Cut by the Gleason Method, *ASME Journal of Mechanical Design*, **115** (1993), pp. 483–489.

[4] GOSSELIN, C. J. – GUERTIN, T. – REMOND, D. – JEAN, Y., Simulation and Experimental Measurement of the Transmission Error of Real Hypoid Gears Under Load, *ASME Journal of Mechanical Design*, **122** (2000), pp. 109–122.

[5] HANDSCHUH, R. F. – BIBEL, G. B., Experimental and Analytical Study of Aerospace Spiral Bevel Gear Tooth Fillet Stresses, *ASME Journal of Mechanical Design*, **121** (1999), pp. 565–572.

[6] KAVASAKI, K. – TAMURA, H. – NAKANO, Y., A Method for Inspection of Spiral Bevel Bears in Klingelnberg Cyclo-Palloïd System, *Proc. of the 1994 International Gearing Conference*, Newcastle upon Tyne, 1994, pp. 305–310.

[7] LELKES, M. – PLAY, D. – MÁRIALIGETI, J., Ívelt fogazatú kúpkerekek érintkezési viszonyainak numerikus analízise. (Numerical Analysis of Contact Conditions for Spiral Bevel Gears), *Gép*, **51** No. 10 (2000), pp. 37–42. (In Hungarian).

[8] LELKES, M. – PLAY, D. – MÁRIALIGETI, J., Cutting Parameters Definition for Klingelnberg Spiral Bevel Gears Optimization, *Proc. of the JSME International Conference on Motion and Power Transmissions MPT2001-Fukuoka*, Fukuoka, November 15–17, 2001, **1**, pp. 375–380.

[9] LITVIN, F. L., *Theory of Gearing*, NASA Reference Publication 1212, 1989.

[10] LITVIN, F. L. – WANG, J. C. – HANDSCHUH, R. F., Computerized Design and Analysis of Face-Milled, Uniform Tooth Height Spiral Bevel Gears Drives, *ASME Journal of Mechanical Design*, **118** (1996), pp. 573–579.

[11] MÁRIALIGETI, J. – CSEKE, J. – LELKES, M., Connection of Some Cutting Parameters with Tooth Surface Modification in Case of Epicycloidal Spiral Bevel Gears, *Proc. of Second Conference on Mechanical Engineering*, Budapest, May 25–26, 2000, **2**, pp. 587–591.

[12] POPPER, GY. – CSIZMÁS, F., *Numerical Methods for Engineers*, Typotex-Akadémiai Kiadó, 1993, pp. 163–164, in Hungarian.

[13] REMOND, D. – PLAY, D., Advantages and Perspectives of Gear Transmission Error Measurements with Optical Encoders, *Proc. of 4*$^{\text{th}}$ *CMET Conference*, Paris, 1999, pp. 199–210.

[14] STADTFELD, H. J. – GAISER, U., The Ultimate Motion Graph, *ASME Journal of Mechanical Design*, **122** (2000), pp. 317–322.

[15] ZHANG, Y. – LITVIN, F. L. – HANDSCHUH, R. F., Computerised Design of Low-Noise Face-Milled Spiral Bevel Gears, *Mechanism and Machine Theory*, **30** No. 8 (1995), pp. 1171–1178.

[16] ZHANG, Y. – LITVIN, F. L. – MARUYAMA, N. – TAKEDA, R. – SUGIMOTO, M., Computerised Analysis of Meshing and Contact of Real Tooth Surfaces, *ASME Journal of Mechanical Design*, **116** (1994), pp. 677–682.